On the Aromaticity of Square Planar Ga_4^{2-} and In_4^{2-} in Gaseous $NaGa_4^-$ and $NaIn_4^-$ Clusters

ARTICLE *in* JOURNAL OF THE AMERICAN CHEMICAL SOCIETY · AUGUST 2001

Impact Factor: 12.11 · DOI: 10.1021/ja0106117 · Source: PubMed

4 AUTHORS, INCLUDING:

Aleksey E. Kuznetsov
Universidade Federal de São Carlos
68 PUBLICATIONS **2,107** CITATIONS
SEE PROFILE

Alexander I Boldyrev
Utah State University
341 PUBLICATIONS **9,994** CITATIONS
SEE PROFILE

Lai-Sheng Wang
Brown University
465 PUBLICATIONS **19,894** CITATIONS
SEE PROFILE

On the Aromaticity of Square Planar Ga_4^{2-} and In_4^{2-} in Gaseous $NaGa_4^-$ and $NaIn_4^-$ Clusters

Aleksey E. Kuznetsov,[†] Alexander I. Boldyrev,*[,†] Xi Li,[‡,§] and Lai-Sheng Wang*[,‡,§]

Contribution from the Department of Chemistry and Biochemistry, Utah State University, Logan, Utah 84322, Department of Physics, Washington State University, 2710 University Drive, Richland, Washington 99352, and W. R. Wiley Environmental Molecular Sciences Laboratory, Pacific Northwest National Laboratory, MS K8-88, P.O. Box 999, Richland, Washington 99352

Received March 7, 2001

Abstract: We investigated the electronic structure and chemical bonding of two bimetallic clusters $NaGa_4^-$ and $NaIn_4^-$. Photoelectron spectra of the anions were obtained and compared with ab initio calculations. We found that the ground state of the two anions contains a square planar dianion interacting with a Na^+ cation. The Ga_4^{2-} and In_4^{2-} dianions both possess two delocalized π electrons and are considered to be aromatic, similar to that recently found in Al_4^{2-}. Using calculations for a model compound, we showed that a recently synthesized Ga_4−organometallic compound also contains an aromatic $-Ga_4^{2-}-$ unit, analogous to the gaseous clusters.

Introduction

Metals and organic compounds represent opposite sides in chemistry and their physical and chemical properties are very different. However, in recent years some metallic properties such as electric conductivity[1] and even superconductivity[2] have been observed in organic materials. Yet, there has been little effort in designing pure metallic compounds possessing organic properties. One of the properties usually referred to organic compounds is aromaticity. Although aromaticity has been extended to include heterosystems[3−5] and organometallic compounds,[6−8] it has not been considered in pure all-metal species until very recently. We have investigated MAl_4^- (M = Li, Na, and Cu) and reported evidence of aromaticity in these purely metallic systems.[9] These bimetallic clusters were found to possess an M^+ cation interacting with a square planar Al_4^{2-}, which is a two π-electron all-metal aromatic species. We further extended the all-metal aromatic idea from Al_4^{2-} into a series of heteroclusters, XAl_3^- (X = Si, Ge, Sn, and Pb).[10] We provided both experimental and theoretical evidence that all the XAl_3^- species have two lowest energy singlet isomers: a four-membered heterocyclic structure (C_{2v}) and a trigonal pyramidal structure (C_{3v}). The heterocyclic structure was found to be the ground state with the pyramidal species as a low-lying isomer. But the relative stability of the heterocyclic ground state was found to increase relative to the pyramidal isomer for the XAl_3^- species with heavier heteroatoms. The heterocyclic XAl_3^- isomer, which is isoelectronic with Al_4^{2-}, was found to be aromatic with two π-electrons. However, the lightest congener of the XAl_3^- series, CAl_3^-, was previously found to have a C_{3v} structure;[11] the aromatic cyclic structure is not even a minimum for CAl_3^-. Thus we observed that the aromatic stabilization becomes more important the more metallic the XAl_3^- heterosystem is.

To further explore aromaticity in all-metal species, here we investigate the heavier congeners of the aromatic Al_4^{2-}: Ga_4^{2-} and In_4^{2-}. Bimetallic anionic clusters with chemical compositions of $NaGa_4^-$ and $NaIn_4^-$ were created in the gas phase and their electronic energy spectra were obtained with photoelectron spectroscopy. Ab initio calculations showed that both $NaGa_4^-$ and $NaIn_4^-$ possess a C_{4v} pyramidal structure with a Na^+ cation interacting with a square planar dianion, analogous to the MAl_4^- species. Both Ga_4^{2-} and In_4^{2-} are shown to be aromatic with two π-electrons. We further carried out calculations on a model compound, $K_2Ga_4(C_6H_5)_2$, for a recently synthesized organogallium compound, $K_2[Ga_4(C_6H_3\text{-}2,6\text{-}Trip_2)_2]$ (Trip = C_6H_2-2,4,6-iPr_3), which contains a nearly square planar Ga_4 unit bound to the two bulky ligands and stabilized by the two K atoms.[12] Through a detailed molecular orbital (MO) analysis, we showed that the synthetic compound in fact contains an aromatic $-Ga_4^{2-}-$ unit (with two π-electrons) interacting with two K^+ ions, analogous to our bare Ga_4^{2-} species in $NaGa_4^-$, despite the additional coordination in the synthetic compound.

Experimental Method and Results

Details of the experimental setup have been described previously.[13] The $NaGa_4^-$ ($NaIn_4^-$) anions were produced by laser vaporization of a

[†] Utah State University.
[‡] Washington State University.
[§] Pacific Northwest National Laboratory.

(1) Chiang, C. K.; Fincher, C. R.; Park, Y. W.; Heeger, A. J.; Shirakawa, H.; Louis, E. J.; Gau, S. C.; MacDiarmid, A. G. *Phys. Rev. Lett.* **1977**, *39*, 1098.
(2) Jerome, D.; Schulz, H. J. *Adv. Phys.* **1982**, *31*, 299.
(3) van Zandwijk, G.; Janssen, R. A. J.; Buck, H. M. *J. Am. Chem. Soc.* **1990**, *112*, 4155.
(4) Schleyer, P. v. R.; Jiao, H.; van E. Hommes, N. J. R.; Malkin, V. G.; Malkina, O. L. *J. Am. Chem. Soc.* **1997**, *119*, 12669.
(5) Minkin, V. I.; Glukhovtsev, M. N.; Simkin, B. Y. *Aromaticity and Antiaromaticity*; Wiley: New York, 1994.
(6) Li, X. W.; Pennington, W. T.; Robinson, G. H. *J. Am. Chem. Soc.* **1995**, *117*, 7578.
(7) Li, X. W.; Xie, Y.; Schreiner, P. R.; Gripper, K. D.; Crittendon, R. C.; Campana, C. F.; Schaefer, H. F.; Robinson, G. H. *Organometallics* **1996**, *15*, 3797.
(8) Robinson, G. H. *Acc. Chem. Res.* **1999**, *32*, 773.
(9) Li, X.; Kuznetsov, A. E.; Zhang, H. F.; Boldyrev, A. I.; Wang, L. S. *Science* **2001**, *291*, 859.
(10) Li, X.; Zhang, H. F.; Wang, L. S.; Kuznetsov, A. E.; Cannon, N. A.; Boldyrev, A. I. *Angew. Chem., Int. Ed.* **2001**, *40*, 1867.
(11) Boldyrev, A. I.; Simons, J.; Li, X.; Chen, W.; Wang, L. S. *J. Chem. Phys.* **1999**, *110*, 8980.
(12) Twamley, B.; Power, P. P. *Angew. Chem., Int. Ed.* **2000**, *39*, 3500.

10.1021/ja0106117 CCC: $20.00
Published on Web 08/16/2001

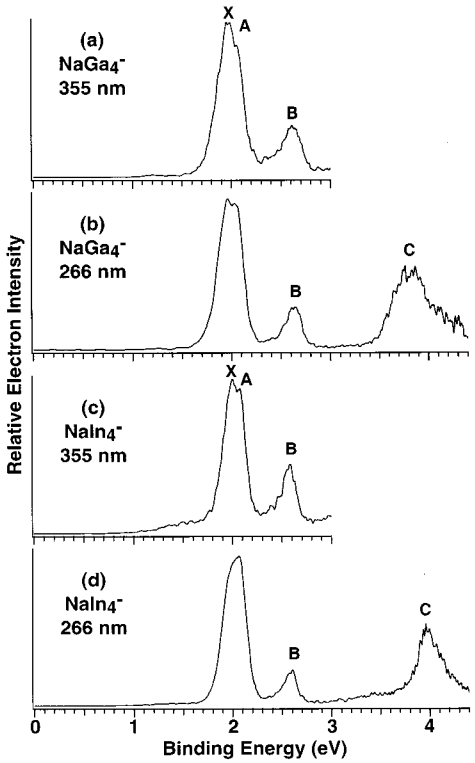

Figure 1. Photoelectron spectra of $NaGa_4^-$ at (a) 355 (3.496 eV) and (b) 266 nm (4.661 eV) and of $NaIn_4^-$ at (c) 355 and (d) 266 nm.

composite target made from Ga (In) and Na_2CO_3. The anionic species from the cluster source were analyzed by using a time-of-flight mass spectrometer. The anions of interest were selected and decelerated before being subjected to photodetachment. Photoelectron spectra of $NaGa_4^-$ and $NaIn_4^-$ (Figure 1) were taken at two detachment laser wavelengths, 355 and 266 nm, and were calibrated by using the known spectra of Cu^-. The photoelectron energy resolution was about 25 meV for 1 eV electrons. The spectra of the two species are similar, each with an intense threshold peak (*X* and *A*), followed by a weak peak (*B*) and a relatively broad feature (*C*). The vertical electron detachment energies (VDEs) of the four spectral features measured from the peak maxima are listed in Table 1 and are compared to ab initio calculations, as discussed below.

Theoretical Methods and Results

We initially optimized geometries and calculated frequencies of $NaGa_4^-$, $NaIn_4^-$, Ga_4^{2-}, and In_4^{2-} (Figure 2) using analytical gradients with polarized split-valence basis sets (6-311+G*)[14−16] for Ga and Na and the relativistic effective core potential with 121G basis sets extended by a set of s, p, and d diffuse functions (CEP-121G+spd)[17−19] for In and Na and a hybrid method known in the literature as B3LYP.[20−22] To test the convergence of our computational results we further studied $NaGa_4^-$ and Ga_4^{2-} using the second-order Moller−Plesset perturbation theory (MP2)[23] and coupled-cluster method [CCSD(T)][24−26] with the 6-311+G* basis sets. The energies of the most stable $NaGa_4^-$ structures were refined by using the CCSD(T) method and the more extended 6-311+G(2df) basis sets. The vertical electron detachment energies were calculated by using the outer valence Green Function method[27−31] [OVGF/6-311+G(2df)] at the CCSD(T)/6-311+G* geometries for $NaGa_4^-$ and OVGF/CEP-121G+spd at the B3LYP/CEP-121G+spd geometries for $NaIn_4^-$. The K_2Ga_4 and $K_2Ga_4(C_6H_5)_2$ model systems were also optimized at the B3LYP level of theory by using the relativistic effective core potential with the LANL2DZ basis set.[32−34] All calculations were performed by using the Gaussian 98 program.[35] MOs for Ga_4^{2-}, $NaGa_4^-$, and Na_2Ga_4, as shown in Figure 3, were calculated at the RHF/6-311+G* level of theory. MOs for K_2Ga_4 and $K_2Ga_4(C_6H_5)_2$, as shown in Figure 4, were calculated at the RHF/LANL2DZ level of theory. All MO pictures were made by using the MOLDEN 3.4 program.[36]

Table 1. Experimental and Theoretical Vertical Electron Detachment Energies (VDE) in eV for $NaGa_4^-$ and $NaIn_4^-$

exptl features	exptl VDE	C_{4v} MO	C_{4v} VDE (theor)	C_{2v} MO	C_{2v} VDE (theor)
		$NaGa_4^-$			
X	1.90 ± 0.06	$3a_1$	1.84 (0.87)[a]	$1b_1$	1.75 (0.85)[a]
A	2.02 ± 0.05	$1b_1$	1.99 (0.85)[a]	$4a_1$	1.80 (0.86)[a]
B	2.58 ± 0.05	$2a_1$	2.43 (0.86)[a]	$3a_1$	2.29 (0.86)[a]
C	3.73 ± 0.15	$1b_2$	3.59 (0.84)[a]	$2b_2$	3.51 (0.83)[a]
		$NaIn_4^-$			
X	1.93 ± 0.06	$3a_1$	1.82 (0.87)[b]	$1b_1$	1.70 (0.85)[b]
A	2.08 ± 0.06	$1b_1$	1.93 (0.86)[b]	$4a_1$	1.78 (0.87)[b]
B	2.60 ± 0.05	$2a_1$	2.39 (0.87)[b]	$3a_1$	2.29 (0.87)[b]
C	3.95 ± 0.15	$1b_2$	3.84 (0.83)[b]	$2b_2$	3.77 (0.83)[b]

[a] The VDEs were calculated at the OVGF/6-311+G(2df) level of theory. The numbers in parentheses indicate the pole strength, which characterizes the validity of the one-electron detachment picture. The detachment processes from the $1b_1$ and $3a_1$ orbitals for the C_{4v} isomer are too close in energy and their order cannot be definitely established in our calculations. [b] The VDEs were calculated at the OVGF/CEP-121G+spd level of theory. The numbers in parentheses indicate the pole strength, which characterizes the validity of the one-electron detachment picture. The detachment processes from the $1b_1$ and $3a_1$ orbitals for the C_{4v} isomer are too close in energy and their order cannot be definitely established in our calculations.

(13) Wang, L. S.; Cheng, H. S.; Fan, J. *J. Chem. Phys*. **1995**, *102*, 9480. Wang, L. S.; Wu, H. In *Advances in Metal and Semiconductor Clusters. IV. Cluster Materials*; Duncan, M. A., Eds.; JAI Press: Greenwich, 1998, p 299.
(14) McLean, A. D.; Chandler, G. S. *J. Chem. Phys*. **1980**, *72*, 5639.
(15) Clark, T.; Chandrasekhar, J.; Spitznagel, G. W.; Schleyer, P. v. R. *J. Comput. Chem*. **1983**, *4*, 294.
(16) Frisch, M. J.; Pople, J. A.; Binkley, J. S. *J. Chem. Phys*. **1984**, *80*, 3265.
(17) Stevens, W. J.; Basch, H.; Krauss, J. *J. Chem. Phys.* **1984**, *81*, 6026.
(18) Stevens, W. J.; Krauss, J.; Basch, H.; Jasien, P. G. *Can. J. Chem*. **1992**, *70*, 612.
(19) Cundari, T. R.; Stevens, W. J. *J. Chem. Phys*. **1993**, *98*, 5555.
(20) Parr, R. G.; Yang, W. *Density-functional theory of atoms and molecules*; Oxford University Press: Oxford, 1989.
(21) Becke, A. D. *J. Chem. Phys.* **1993**, *98*, 5648.
(22) Perdew, J. P.; Chevary, J. A.; Vosko, S. H.; Jackson, K. A.; Pederson, M. R.; Singh, D. J.; Fiolhais, C. *Phys. Rev. B* **1992**, *46*, 6671.
(23) Krishnan, R.; Binkley, J. S.; Seeger, R.; Pople, J. A. *J. Chem. Phys.* **1980**, *72*, 650.
(24) Cizek, J. *Adv. Chem. Phys*. **1969**, *14*, 35.
(25) Purvis, G. D., III; Bartlett, R. J. *J. Chem. Phys*. **1982**, *76*, 1910.
(26) Scuseria, G. E.; Janssen, C. L.; Schaefer, H. F., III *J. Chem. Phys*. **1988**, *89*, 7282.
(27) Cederbaum, L. S. *J. Phys. B* **1975**, *8*, 290.
(28) von Niessen, W.; Shirmer, J.; Cederbaum, L. S. *Comput. Phys. Rep.* **1984**, *1*, 57.
(29) Zakrzewski, V. G.; von Niessen, W. *J. Comput. Chem*. **1993**, *14*, 13.
(30) Zakrzewski, V. G.; Ortiz, J. V. *Int. J. Quantum Chem.* **1995**, *53*, 583.
(31) For a recent review see: Ortiz, J. V.; Zakrzewski, V. G.; Dolgunitcheva, O. In *Conceptual Trends in Quantum Chemistry*; Kryachko, E. S., Ed.; Kluver, Dordrecht, The Netherlands, 1997; Vol. 3, p 463.
(32) Hay, P. J.; Wadt, W. R. *J. Chem. Phys.* **1985**, *82*, 270.
(33) Wadt, W. R.; Hay, P. J. *J. Chem. Phys*. **1985**, *82*, 284.
(34) Hay, P. J.; Wadt, W. R. *J. Chem. Phys*. **1985**, *82*, 299.
(35) M. J. Frisch, G. M. Trucks, H. B. Schlegel, G. E. Scuseria, M. A. Robb, J. R. Cheeseman, V. G. Zakrzewski, J. A. Montgomery, Jr., R. E. Stratmann, J. C. Burant, S. Dapprich, J. M. Millam, A. D. Daniels, K. N. Kudin, M. C. Strain, O. Farkas, J. Tomasi, V. Barone, M. Cossi, R. Cammi, B. Mennucci, C. Pomelli, C. Adamo, S. Clifford, J. Ochterski, G. A. Petersson, P. Y. Ayala, Q. Cui, K. Morokuma, D. K. Malick, A. D. Rabuck, K. Raghavachari, J. B. Foresman, J. Cioslowski, J. V. Ortiz, A. G. Baboul, B. B. Stefanov, G. Liu, A. Liashenko, P. Piskorz, I. Komaromi, R. Gomperts, R. L. Martin, D. J. Fox, T. Keith, M. A. Al-Laham, C. Y. Peng, A. Nanayakkara, C. Gonzales, M. Challacombe, P. M. W. Gill, B. G. Johnson, W. Chen, M. W. Wong, J. L. Andres, M. Head-Gordon, E. S. Replogle, J. A. Pople; *Gaussian 98*, Revision A.7; Gaussian, Inc.: Pittsburgh, PA, 1998.
(36) Schaftenaar, G. MOLDEN3.4, CAOS/CAMM Center, The Netherlands, 1998.

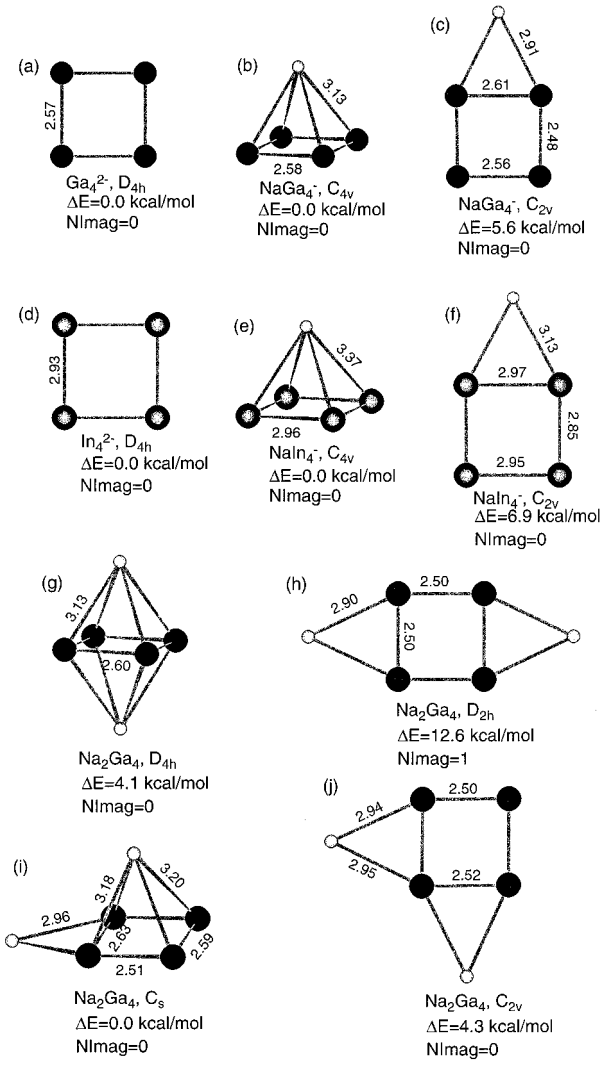

Figure 2. Optimized structures of (a) Ga_4^{2-} (D_{4h}), (b) $NaGa_4^-$ (C_{4v}), and (c) $NaGa_4^-$ (C_{2v}) at the B3LYP/6-311+G* level of theory; (d) In_4^{2-} (D_{4h}), (e) $NaIn_4^-$ (C_{4v}), and (f) $NaIn_4^-$ (C_{2v}) at B3LYP/CEP-121G+spd level of theory; and (g) Na_2Ga_4 (D_{4h}), (h) Na_2Ga_4 (D_{2h}), (i) Na_2Ga_4 (C_s), and (j) Na_2Ga_4 (C_{2v}) at the B3LYP/6-311+G* level of theory. Bond lengths are given in Å.

Exhaustive searches for the global minima of Al_4^{2-}, $NaAl_4^-$, and Na_2Al_4 were performed in our previous work.[9] For Al_4^{2-} we found that the planar square structure is the most stable. For $NaAl_4^-$, two low-lying singlet structures were found: a C_{4v} pyramidal and a C_{2v} planar structure. For Na_2Al_4 we located four low-lying singlet structures: a D_{4h} bipyramidal, a D_{2h} planar, a C_{2v} planar, and a C_s structure. We expected that Ga_4^{2-} (In_4^{2-}), $NaGa_4^-$ ($NaIn_4^-$), and Na_2Ga_4 (Na_2In_4) should have similar structures and isomers as Al_4^{2-}, $NaAl_4^-$, and Na_2Al_4, respectively, and hence we considered here the same sets of structures for these heavier species.

The optimized geometries, vibrational frequencies, and relative energies of Ga_4^{2-} and the two lowest structures of $NaGa_4^-$ are given in Tables 2−4, respectively, at the B3LYP/6-311+G*, MP2/6-311+G*, and CCSD(T)/6-311+G* levels of theory. The agreement among the three theoretical methods is very good, considering the softness of the potential energy surfaces. More importantly, the consistency among the three levels of theory suggests that we can use reliably the B3LYP method for larger systems. For $NaGa_4^-$ and $NaIn_4^-$ the global minimum C_{4v} pyramidal structure (Figure 2b and 2e) was found to be more stable than the C_{2v} planar structure (Figure 2c and 2f) by 6.9 (CCSD(T)/6-311+G(2df)) and 6.9 kcal/mol (B3LYP/CEP-121G+spd), respectively.

For Na_2Ga_4 the global minimum structure (Figure 2i) has C_s symmetry with one sodium cation coordinated to the edge and the other one located above the planar structure of the Ga_4^{2-} dianion. This is consistent with our previous Na_2Al_4 results.[9] While the structure of the Ga_4^{2-} dianion in Na_2Ga_4 is somewhat distorted from a perfect square, the distortion is very modest and the geometric integrity of the aromatic dianion is clearly seen. The bipyramidal structure with the two cations above and below the Ga_4^{2-} planar unit (Figure 2g) was found to be a local minimum 4.1 kcal/mol higher in energy than the global minimum. Two planar structures were found to be a first-order saddle point (Figure 2h) 12.6 kcal/mol higher in energy and a local minimum (Figure 2j) 4.3 kcal/mol higher in energy, all at B3LYP/6-311+G*. Again for these two isomers, the geometric integrity of the Ga_4^{2-} dianion is clearly seen with very slight distortions.

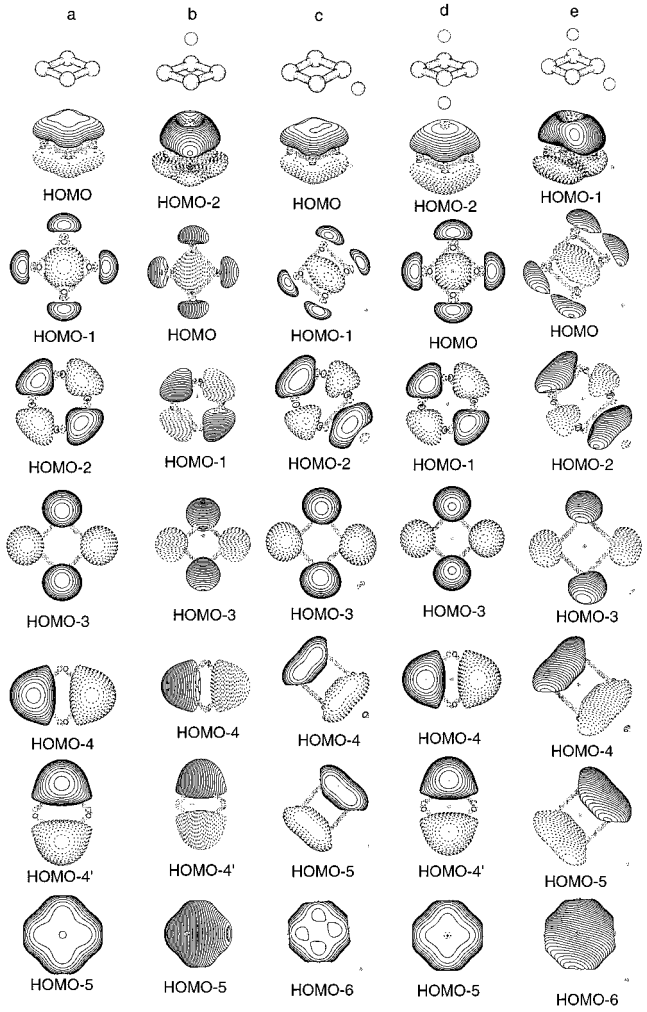

Figure 3. Molecular structure and molecular orbital pictures of (a) bare Ga_4^{2-}, (b) C_{4v} $NaGa_4^-$, (c) C_{2v} $NaGa_4^-$, (d) D_{4h} Na_2Ga_4, and (e) C_s Na_2Ga_4.

Interpretation of the Experimental Results and Confirmation of the Pyramidal Ground-State Structure of $NaGa_4^-$ and $NaIn_4^-$

Theoretical calculations of the four lowest lying vertical one-electron detachment processes for the C_{2v} planar and C_{4v} pyramidal species of $NaGa_4^-$ and $NaIn_4^-$ were performed and are compared with the experimental VDEs in Table 1. The pole strengths, given in parentheses in Table 1, are larger than 0.8 for all the calculated detachment channels, implying that the OVGF method is expected to be valid and all the electron detachment channels can be considered as primarily one-electron processes. Excellent agreement was obtained for the two anions between the predicted VDEs of the C_{4v} pyramidal structures and the experimental data and will be discussed in more detail below, whereas those for the low-lying C_{2v} planar isomers do

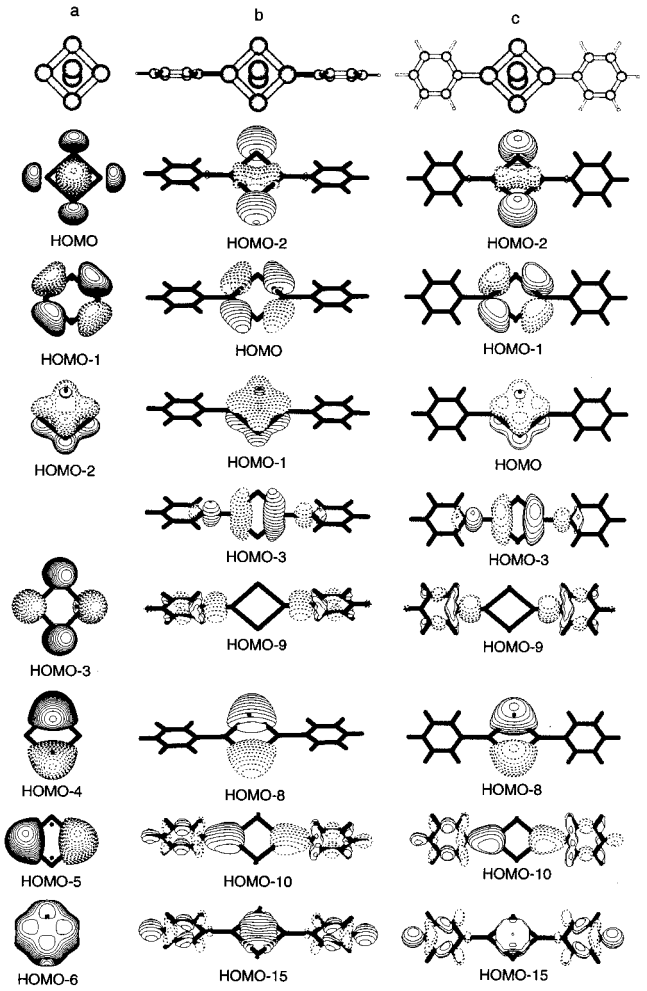

Figure 4. Molecular structure and molecular orbital pictures of (a) K_2Ga_4, (b) $K_2Ga_4(C_6H_5)_2$ with the Ga_4 ring perpendicular to the two phenyl groups, and (c) $K_2Ga_4(C_6H_5)_2$ with the Ga_4 ring in the same plane as the two phenyl groups.

Table 2. Calculated Molecular Properties of Ga_4^{2-}

	D_{4h}, $^1A_{1g}$		
	B3LYP/ 6-311+G*	MP2/ 6-311+G*	CCSD(T)/ 6-311+G*
R(Ga−Ga), Å	2.566	2.599	2.618
E_{tot}, au	−7699.49103	−7693.06316	−7693.08947
$\omega_1(a_{1g})$, cm^{-1}	182	199	
$\omega_2(b_{1g})$, cm^{-1}	101	72	
$\omega_3(b_{2g})$, cm^{-1}	175	176	
$\omega_4(b_{2u})$, cm^{-1}	75	75	
$\omega_5(e_u)$, cm^{-1}	164	201	

not agree well with the experiment. The photoelectron spectra of $NaGa_4^-$ and $NaIn_4^-$ are nearly identical and will be discussed together. The similar photoelectron spectra of the two species are consistent with their similar structure and bonding born out of our theoretical predictions.

Bands *X* and *A*. The ground-state feature (*X*, Figure 1) peaking at 1.90 ($NaGa_4^-$) and 1.93 eV ($NaIn_4^-$) agrees well with the calculated VDE of 1.84 eV for $NaGa_4^-$ at OVGF/6-311+G(2df) and that of 1.82 eV for $NaIn_4^-$ at OVGF/CEP-121+spd from detachment of an electron from the $3a_1$-HOMO of the global minimum structures (Table 1). The $3a_1$-HOMO is a σ-bonding MO formed from the radial p-orbitals of Ga or In (Figure 3). The next higher binding feature (*A*) is closely spaced from the ground-state detachment feature (*X*), but was well resolved in the 355 nm spectra for both species. The second vertical electron detachment takes place from the $1b_1$ orbital (HOMO-1) with a theoretical VDE of 1.99 eV for $NaGa_4^-$ [OVGF/6-311+G(2df)] and 1.93 eV for $NaIn_4^-$ [OVGF/CEP-121+spd] (Table 1). These values agree well with the second detachment feature (*A*), which was observed at 2.02 ($NaGa_4^-$) and at 2.08 eV ($NaIn_4^-$), as seen clearly in Figure 1. The $1b_1$ orbital is also a σ-bonding MO formed from the perpendicular p-orbitals of Ga or In (Figure 3).

Table 3. Calculated Molecular Properties of the Pyramidal Structure of $NaGa_4^-$

	C_{4v}, $^1A_1$		
	B3LYP/ 6-311+G*	MP2/ 6-311+G*	CCSD(T)/ 6-311+G*
R(Ga−Ga), Å	2.580	2.618	2.631
R(Na−Ga), Å	3.134	3.145	3.181
E_{tot}, au	−7861.89147	−7855.02418	−7855.05512[a]
$\omega_1(a_1)$, cm^{-1}	184	193	
$\omega_2(a_1)$, cm^{-1}	159	165	
$\omega_3(b_1)$, cm^{-1}	185	182	
$\omega_4(b_2)$, cm^{-1}	111	110	
$\omega_5(b_2)$, cm^{-1}	90	87	
$\omega_6(e)$, cm^{-1}	160	194	
$\omega_7(e)$, cm^{-1}	69	78	

[a] Frequencies have not been calculated at this level of theory.

Table 4. Calculated Molecular Properties of the Planar Structure of $NaGa_4^-$

	C_{2v}, $^1A_1$		
	B3LYP/ 6-311+G*	MP2/ 6-311+G*	CCSD(T)/ 6-311+G*
$R(Ga_b-Ga_b)$, Å	2.611	2.666	2.675
$R(Ga_b-Ga_t)$, Å	2.480	2.529	2.535
$R(Ga_t-Ga_t)$, Å	2.563	2.608	2.603
$R(Na-Ga_b)$, Å	2.914	2.967	3.181
E_{tot}, au	−7861.88219	−7855.01548	−7855.04380[a]
$\omega_1(a_1)$, cm^{-1}	228	228	
$\omega_2(a_1)$, cm^{-1}	185	189	
$\omega_3(a_1)$, cm^{-1}	175	178	
$\omega_4(a_1)$, cm^{-1}	143	157	
$\omega_5(a_2)$, cm^{-1}	77	79	
$\omega_6(b_1)$, cm^{-1}	24	38	
$\omega_7(b_2)$, cm^{-1}	201	239	
$\omega_8(b_2)$, cm^{-1}	109	117	
$\omega_9(b_2)$, cm^{-1}	61	57	

[a] Frequencies have not been calculated at this level of theory.

Band *B*. The third detachment feature (*B*) is relatively weak and well-separated from feature *A*. This feature should correspond to removal of an electron from the $2a_1$ (HOMO-2) orbital with a theoretical VDE of 2.43 eV for $NaGa_4^-$ [OVGF/6-311+G(2df)] and 2.39 eV for $NaIn_4^-$ [OVGF/CEP-121+spd]. The theoretical VDEs for this detachment channel agree well with the third detachment feature (*B*), which was observed at a VDE of 2.58 eV for $NaGa_4^-$ and 2.60 eV for $NaIn_4^-$. The $2a_1$-MO (HOMO-2) is a π-bonding orbital formed from the out-of-plane p-orbitals of Ga or In (Figure 3).

Band *C*. The fourth detachment band (*C*) has a much higher electron binding energy and appears to be quite broad, in particular for the spectrum of $NaGa_4^-$ (Figure 1b). This detachment feature should be due to removal of an electron from the $1b_2$ MO (HOMO-3) with a theoretical VDE of 3.59 eV for $NaGa_4^-$ [OVGF/6-311+G(2df)] and 3.84 eV for $NaIn_4^-$ [OVGF/CEP-121+spd]. These values are in good agreement with the third detachment feature (*C*), which was observed at VDEs of 3.73 and 3.95 eV for $NaGa_4^-$ and $NaIn_4^-$, respectively. The $1b_2$ MO (HOMO-3, Figure 3) is an antibonding orbital formed from the 3s atomic orbitals of Ga or In, which is why it has a

much higher electron binding energy in both species. The broad width of the fourth detachment feature is also consistent with the antibonding character of the $1b_2$ orbital (Figure 3).

The overall agreement between the experimental photoelectron spectra and the theoretical calculations is quite satisfying. The excellent agreement between the calculated VDEs of the C_{4v} structure and the experimental VDEs unequivocally confirmed that the C_{4v} structure is the ground state for both anions. The VDEs of the C_{2v} low-lying isomers are all lower than those of the C_{4v} ground-state anions (Table 1) and are in much poorer agreement with the measured experimental VDEs. In fact, the very weak lower binding energy tails discernible in the photoelectron spectra (Figure 1) may be due to contributions from the C_{2v} isomers.

Aromaticity of Ga_4^{2-} and In_4^{2-} in Their Isolated State and Inside the $NaGa_4^-$, $NaIn_4^-$, Na_2Ga_4, and Na_2In_4 Bimetallic Clusters

Before discussing aromaticity in the Ga and In species, we first comment on the use of doubly charged anions to understand the structure and bonding of the bimetallic clusters, even though the doubly charged anions may not be electronically stable as isolated species. It should be pointed out that the majority of common inorganic multiply charged anions are not electronically stable as isolated species due to the strong Coulomb repulsion among the excess charges in the isolated state.[37] Probably the best known example is the SO_4^{2-} dianion, which is considered to be a building block of all sulfate compounds. Yet it is not electronically stable in the gas phase[38,39] and requires either a counterion or at least three water molecules to be stabilized.[40,41] Nevertheless, the instability as an isolated dianion does not preclude SO_4^{2-} as a ubiquitous building block in inorganic materials and solutions and it acquires its stability in the condensed phase through counterions or solvents. Furthermore, highly charged anions, such as those found in the Zintl phase, are very common in intermetallic materials and are important in understanding the structure and bonding in these solids.[42,43] Another example among organic species is the doubly charged $H_4C_4^{2-}$ ion, which was first predicted computationally[44,45] to be aromatic, despite the fact that it is not a stable gaseous species. As a matter of fact, an analogue of this unstable dianion has been successfully synthesized recently, in which the H atoms were substituted by bulky $Si(CH_3)_3$ ligands.[46] Certainly, countercations or solvent molecules play an important role in the stabilization of these multiply charged species, but it is the electronic and structural integrity of the multiply charged species that is crucial for them to be important building blocks and valuable models to understand the properties of materials containing them.

The MOs of Ga_4^{2-}, the two most stable structures of $NaGa_4^-$, and the two most stable structures of Na_2Ga_4 are compared in Figure 3. One can see that the role of Na^+ is to stabilize an otherwise electronically unstable Ga_4^{2-} dianion and it has relatively minor effects on the electronic structure of the dianion. The same sets of MOs are present in all species regardless of the coordination places of the countercations, even though the order of the first three occupied MOs is slightly varied.

The HOMO ($1a_{2u}$) of Ga_4^{2-} is formed from the out-of-plane 4p orbitals (Figure 3a). The HOMO-1 ($2a_{1g}$) and HOMO-2 ($1b_{2g}$) are bonding orbitals formed from the in-plane 4p orbitals. The following four MOs are bonding, nonbonding, and antibonding orbitals formed from the filled valence 4s orbitals of Ga. When all bonding, nonbonding, and antibonding MOs composed of the same atomic orbitals (such as the 4s orbitals of Ga in this case) are occupied, the net bonding effect is zero and the atomic orbitals can be viewed as lone pairs. This fact can be understood better by using He_2 as an example. In the He_2 dimer, both bonding ($1s_{He1} + 1s_{He2}$) and antibonding ($1s_{He1} - 1s_{He2}$) MOs are occupied, the net bonding effect is zero, and the 1s orbital at each He atom can be treated as a lone pair.

The HOMO of Ga_4^{2-} is the most interesting orbital, which shows vividly a delocalized π orbital and renders aromaticity to this species. We emphasize that the unique stability and square structure of the Al_4^{2-}, Ga_4^{2-}, and In_4^{2-} species (and we expect it to be also true for Tl_4^{2-}) arise not only from the presence of the fully occupied π-orbital ($1a_{2u}$, HOMO) but also from the two σ-bonding MOs composed of radial p-orbitals ($2a_{1g}$, HOMO-1) and perpendicular (in-plane) p-orbitals ($1b_{2g}$, HOMO-2—a four-center MO) of Al, Ga, or In. It is the complete bonding nature in these three MOs that make these 14-valence-electron species stable and square planar. However, it is the π-MO that gives the agreement with the $(4n + 2)$ Huckel rule and makes it possible to connect to the concept of aromaticity. The two four-center σ MOs also render the M_4^{2-} species σ aromaticity.

In the $NaGa_4^-$ and Na_2Ga_4 species, the MOs of the Ga_4^{2-} dianion can be easily recognized. They are only distorted very slightly by the presence of the cations, showing the electronic integrity of the aromatic dianion. The next criterion for aromaticity is the structural integrity of the dianion inside the $NaGa_4^-$ and Na_2Ga_4 species. As one can see in Figure 2, regardless of the external coordination of one or two cations, the geometry of the Ga_4^{2-} dianion is only modestly distorted and clearly showing its structural integrity. Hence, based on the square planar structure of Ga_4^{2-} and In_4^{2-} (provided by the σ- and π-bonding), their electronic and structural integrity in the Na-bimetallic clusters, and the presence of the two π-electrons satisfying the $(4n + 2)$ Huckel rule, we concluded that both Ga_4^{2-} and In_4^{2-} indeed exhibit characteristics of aromaticity and should be considered to be aromatic, similar to their lighter congener, Al_4^{2-}.

Aromatic Ga_4^{2-} as Building Blocks in Organometallic Compounds

The natural question is whether the newly found all-metal aromatic clusters can be synthesized as building blocks in bulk materials. One promising route to isolate these species would be to prepare them in bulk salt crystals with the X_2M_4 composition with isolated M_4^{2-} units (where X = alkali metals, M = Al−Tl), such as those found in many Zintl phase materials. As Seo and Corbett pointed out previously,[47] the challenge would be to have the M_4^{2-} units completely separated from each other because an incomplete separation may lead to fusion of the M_4^{2-} building blocks to form larger clusters. A second

(37) Boldyrev, A. I.; Gutowski, M.; Simons, J. *Acc. Chem. Res*. **1996**, *29*, 497.
(38) Janoschek, R. *Z. Anorg. Allg. Chem*. **1992**, *616*, 101.
(39) Boldyrev, A. I.; Simons, J. *J. Phys. Chem. A* **1994**, *98*, 2298.
(40) Wang, X. B.; Ding, C. F.; Nicholas, J. B.; Dixon, D. A.; Wang, L. S. *J. Phys. Chem*. A **1999**, *103*, 3423.
(41) Wang, X. B.; Nicholas, J. B.; Wang, L. S. *J. Chem. Phys*. **2000**, *113*, 10837.
(42) Corbett, J. D. *Angew. Chem., Int. Ed*. **2000**, *39*, 670.
(43) *Chemistry, Structure and Bonding of Zintl Phases and Ions*; Kauzlarich, S. M., Ed.; VCH: New York, 1996.
(44) Zandwijk, G. v.; Jansen, R. A.; Buck, H. M. *J. Am. Chem. Soc*. **1990**, *112*, 4155.
(45) Balci, M.; McKee, M. L.; Schleyer, P. v. R. *J. Phys. Chem. A* **2000**, *104*, 1246.
(46) Sekiguchi, A.; Matsuo, T.; Watanabe, H. *J. Am. Chem. Soc*. **2000**, *122*, 5652.
(47) Seo, D.-K.; Corbett, J. D. *Science* **2001**, *291*, 841.

strategy might be to synthesize the M_4^{2-} unit protected by large organic ligands. Remarkably such an organometallic compound containing a Ga_4^{2-} unit may have already been synthesized. Recently Twamley and Power (TP)[12] reported the synthesis and structural characterization of $K_2[Ga_4(C_6H_3\text{-}2,6\text{-}Trip_2)_2]$ (Trip = C_6H_2-2,4,6-^{i}Pr$_3$), consisting of two K^+ coordinated to a square planar Ga_4^{2-} bipyramidally. The Ga_4^{2-} unit in this remarkable compound is bound diagonally to two phenyl carbons from the two ligands. As we will show below from model calculations, the electronic structure of the $-Ga_4^{2-}-$ unit in the TP compound is analogous to that in our $NaGa_4^-$ and Na_2Ga_4 molecules and indeed can be considered to be aromatic. More remarkably, the two ligands of Ga_4^{2-} in the TP compound can be interpreted as an example of substitutions at the lone pair of Ga rather than addition to the π-bond, analogous to the characteristic reactivity of aromatic molecules.

TP thoughtfully rationalized the bonding in the square planar Ga_4 in the $K_2[Ga_4(C_6H_3\text{-}2,6\text{-}Trip_2)_2]$ compound using the classical valence bonding model. They suggested that the two Ga^I atoms that are coordinated by the ligands use their three valence electrons to bond a carbon and the other Ga^{II} atoms, whereas the two Ga^{II} atoms each simply bond to the two Ga^I atoms, completing the square. The two two-coordinated Ga^{II} atoms each have their remaining coordination site occupied by a lone pair (the extra electrons being provided from the charge transfers from the two K atoms, giving rise to the 2− charge on Ga_4). While this is a perfectly reasonable and sound interpretation, the square planar $-Ga_4^{2-}-$ unit in this new compound is highly unusual and intriguing. We performed model calculations to see if the $-Ga_4^{2-}-$ unit in this compound is related to our Ga_4^{2-} in the metallic clusters and more importantly if it is similarly aromatic.

The model system we chose was $K_2Ga_4(C_6H_5)_2$, which was calculated employing the B3LYP/LANL2DZ basis sets and pseudopotentials for the Ga and K atoms. The optimized structures for this model compound together with the square bipyramidal K_2Ga_4 structure are shown in Figure 4 (only MOs pertinent to the Ga_4 core are presented). The nonplanar structure containing a square planar Ga_4 unit perpendicular to the two phenyl groups (Figure 4b) is a second-order saddle point 6.5 kcal/mol higher (B3LYP/LANL2DZ) in energy. The all-planar structure (Figure 4c) is a true minimum, but it is different from the TP compound, where the two phenyl groups are perpendicular to the plane of the $-Ga_4^{2-}-$ unit similar to the model in Figure 4b. We believe that the fact that the phenyl groups are perpendicular to the $-Ga_4^{2-}-$ unit in the TP compound is due to additional interactions of the C_6H_3-2,6-Trip ligands with the K^+ cations. However, as seen in Figure 4, both the planar and perpendicular structures of our model systems have the same sets of MOs for the pertinent Ga_4^{2-} unit. The corresponding MOs of the $K_2Ga_4(C_6H_5)_2$ model systems are compared to those of the bimetallic cluster, K_2Ga_4, in Figure 4. The similarity between them is clearly revealed. The only difference is that s−p hybridizations among the $1a_{1g}$ (HOMO), $1b_{1g}$ (HOMO-3), and one component of the $1e_u$ (HOMO-5) orbitals (the latter two are essentially linear combinations of the 4s orbitals of Ga) occur in the model compounds to accommodate the Ga−C σ bonds. Thus, among the three p-type bonding orbitals in the bare cluster, the radial MO ($2a_{1g}$, HOMO) is being used to accommodate the two Ga−ligand bonds while the π orbital ($1a_{2u}$, HOMO-2) and the 4-center Ga−Ga bonding MO ($1b_{2g}$, HOMO-1) are nearly unchanged in the organometallic compound relative to the bare cluster. Thus, both of these two orbitals must be essential for the square planar structure.

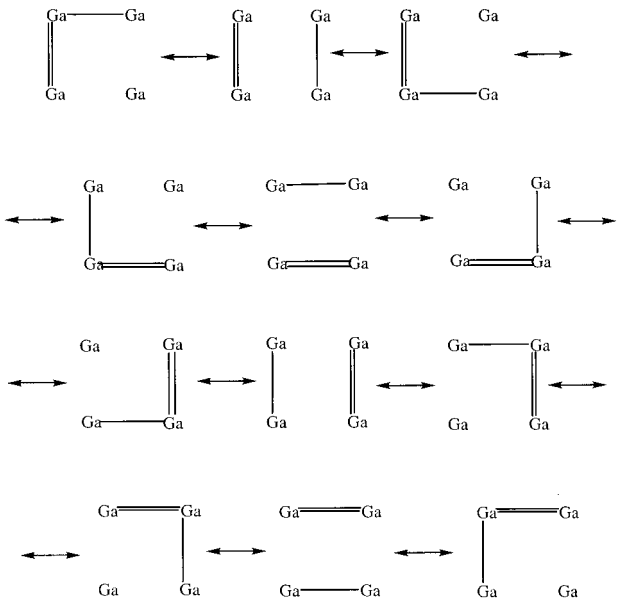

Figure 5. Twelve resonance structures representing bonding in Ga_4^{2-}.

Bonding in the model $K_2Ga_4(C_6H_5)_2$ and the TP compounds can be interpreted as the following (using the MOs shown in Figure 4b): HOMO-2 and HOMO-8 are responsible for the two lone pairs on Ga^{II}, HOMO-9 and HOMO-10 are responsible for the two Ga^I−C σ bonds, HOMO-1 is the four-center π-bond, and HOMO, HOMO-3, and HOMO-15 are responsible for three σ Ga−Ga bonds. Therefore, we conclude that the TP compound indeed contains an aromatic $-Ga_4^{2-}-$ species. It should be noted that organogallium compounds containing a cyclic $-Ga_3^{2-}-$ group have been synthesized and suggested to be aromatic previously.[6−8]

Finally, we like to compare the nature of our aromatic all-metal M_4^{2-} (M = Al, Ga, In) species with a two π-electron organic aromatic species, $H_4C_4^{2+}$.[45] Although all these species possess two π-electrons and are aromatic, they are not isoelectronic. The square planar all-metal systems have 14 valence electrons, while the aromatic $H_4C_4^{2+}$ has 18 valence electrons. The 4 valence electron deficit in our all-metal M_4^{2-} systems has important consequences. In $H_4C_4^{2+}$, there are 8 classical two-center two-electron bonds (the 4 C−H bonds and the 4 C−C bonds), plus one delocalized four-center π-bond that gives rise to the aromaticity of this species.[45] On the other hand, the all-metal M_4^{2-} clusters have only seven pairs of electrons each. Four pairs can be assigned to four lone pairs of M, as discussed earlier. One pair is the delocalized four-center π-bond and only two pairs of electrons are available for σ-bonds. Therefore, one cannot draw the classical structure for M_4^{2-} with four two-center two-electron bonds. These systems are electron deficient. The only possible representation using the classical two-center two-electron language for these systems is through the 12 resonant structures presented in Figure 5 for Ga_4^{2-}. The average M−M bond order in these metallic clusters is only 0.75, resulting from the three bonding MOs (two σ and one π bonds) divided among the four M−M bonds in the M_4^{2-} square.

However, when four monovalent ligands (X) are added to M_4^{2-} to form $X_4M_4^{2-}$, four additional electrons are added to the valent shell and s−p hybridizations occur. The s−p hybridizations make it possible to form four two-center two-electron X−M bonds and four two-center two-electron M−M bonds, still preserving the two-electron four-center π-bond. The additions of the ligands to M_4^{2-} and the resulting s−p hybridization transform M from monovalent in M_4^{2-} to the

normal trivalent M in $X_4M_4^{2-}$.[48] These systems are now valent isoelectronic to the $H_4C_4^{2+}$ hydrocarbon aromatic analogue. The $X_2M_4^{2-}$ dianions, characteristic of the TP compound (M = Ga), have 16 valence electrons and are between the completely "naked" (M_4^{2-}) and completely "dressed" ($X_4M_4^{2-}$) cases and therefore are still electron-deficient systems. While all three cases are two π-electron aromatic systems, their differences are in the number of M−M σ bonds. The M_4^{2-} and $X_2M_4^{2-}$ species only have two and three σ bonds and are short by two and one σ bonds, respectively, relative to the classical description of a M_4 square which needs 4 σ M−M bonds, as is the case in $X_4M_4^{2-}$. Our analyses suggest that similar TP compounds with M = Al, In, and Tl or with four ligands may also be synthesized if appropriate ligands or reaction conditions can be found.

Conclusions

We reported an experimental and theoretical investigation of gaseous $NaGa_4^-$ and $NaIn_4^-$ bimetallic clusters and showed that their bonding can be viewed as a Na^+ cation interacting with a Ga_4^{2-} or In_4^{2-} dianion. We provided experimental and theoretical evidence that the 14 valence electron Ga_4^{2-} and In_4^{2-} are analogous to the recently discovered Al_4^{2-} as in $NaAl_4^-$ and possess the geometrical and electronic properties to be considered as aromatic systems. Furthermore, the analysis of the electronic structure of a $K_2Ga_4(C_6H_5)_2$ model system provided us with evidence to suggest that a recently synthesized $K_2[Ga_4(C_6H_3\text{-}2,6\text{-}Trip_2)_2]$ (Trip = C_6H_2-2,4,6-^{i}Pr$_3$) compound, which contains a nearly square planar Ga_4 unit bound to the two bulky ligands and stabilized by the two K atoms, can be interpreted as having a $-Ga_4^{2-}-$ aromatic unit, analogous to the isolated $NaGa_4^-$ species. It is believed that the current gas-phase studies provide unique electronic and structural information, which is valuable in providing a conceptual framework for understanding the structure and bonding of new materials and compounds, as well as guiding the discoveries of new ones. This work also shows that much is still to be done and gained in advancing the concept of aromaticity in all-metal systems. Species with antiaromaticity, bicyclic structures, two-dimensional aromatic layers, and sandwich structures are yet to be discovered.

Acknowledgment. The theoretical work was done at Utah State University and supported by donors of the Petroleum Research Fund (ACS-PRF No. 35255-AC6), administered by the American Chemical Society. The experimental work done at Washington is supported by the National Science Foundation (DMR-0095828). The experiment was performed at the W. R. Wiley Environmental Molecular Sciences Laboratory, a national scientific user facility sponsored by DOE's Office of Biological and Environmental Research and located at Pacific Northwest National Laboratory, which is operated for DOE by Battelle under Contract DE-AC06-76RLO 1830.

JA0106117

(48) Li, X.; Wu, H.; Wang, X. B.; Wang, L. S. *Phys. Rev. Lett.* **1998**, *81*, 1909.